THE TRANSACTIONS OF THE ROYAL INSTITUTION OF NAVAL ARCHITECTS

Part A – International Journal of Maritime Engineering

EXPERIMENTAL TESTING OF RIVETED CARVEL PLANKS ON FRAMES FOR TRADITIONAL TIMBER STRUCTURES

(DOI No: 10.3940/rina.ijme.2016.a2.???)

J-B R G Souppez*, Aston University, UK
* Corresponding author. J-B R G Souppez (Email) j.souppez@aston.ac.uk

SUMMARY

Traditional wooden boats are characterised by closely spaced frames, riveted to thick planks, leading to high thickness-to-span ratios. However, the effect of such closely spaced frames and thickness-to-span ratio remains uncharacterised. Consequently, four-point bending tests are undertaken to quantify the ultimate flexural strength and flexural modulus of wooden planks with up to 3 frames and thickness-to-span ratios from 0.0267 to 0.200. The results show that (i) a greater number of frames for a given span yields a reduction in specific stiffness but a constant specific strength; (ii) a maximum thickness-to-span ratio of 0.080 and 0.050 is recommended to ensure the strength and stiffness exceed regulatory default properties, respectively, and (iii) additional factors of safety would be needed for traditional construction to be included in existing structural regulations. These findings provide novel insights into the structural design of traditional wooden boats and may contribute to their future inclusion in regulatory frameworks.

KEYWORDS

Carvel construction, Traditional wooden boatbuilding, ISO 12215-5, Structural analysis, Mechanical characterisation.

NOMENCLATURE

b	Width (mm)
B	Bias limit (varies)
B_{H}	Hull beam (m)
D_{H}	Hull depth (m)
E	Flexural modulus (GPa)
F	Force applied to beam sample (N)
h	Beam thickness (mm)
l	Load span (mm)
L_{OA}	Hull length overall (m)
M_{c}	Moisture content (%)
n	Number of repeats (-)
N	Number of independent variables (-)
P	Pressure (MPa)
P_{r}	Precision (varies)
r	Loading-point nose radius (mm)
s	Span between test machine supports (mm)
s_{CL}	Frame spacing (mm)
S_{n}	Gerr scantling number (-)
t	Plating thickness (mm)
T	Temperature (°C)
t_{95}	Student multiplies (-)
U	Uncertainty (varies)
X	Given quantity (varies)
x_i	Given independent variable (varies)
ε	Maximum strain for any value of F (-)
σ	Ultimate flexural stress (MPa)
σ_{d}	Design stress (MPa)
σ_{dev}	Standard deviation (varies)
ρ	Density (kg m^{-3})
φ	Relative humidity (-)
ω	Vertical displacement of cross-head (mm)
ABS	American Bureau of Shipping
GL	Germanischer Lloyd
ISO	International Organization for Standardization

1. INTRODUCTION

Wooden boats have been predominant throughout history (Ward, 2006; Park et al., 2010; McGrail, 2014), prior to the advent of metal (Fairbairn, 1865; Baxter, 1933) and, more recently, composite (Greene, 1990; Souppez, 2018) construction. The significant progress in adhesives associated with the latter (Beck et al., 2010) has led to the development of modern timber construction, namely cold moulding and strip planking, relying on epoxy and modern adhesives for timber encapsulation (Loscombe, 1998; Gougeon, 2005). This alleviates the expansion of timber with increasing moisture content (Birmingham, 1992; Souppez, 2023a), which is defined as the mass of water in timber compared to the dry mass of the timber. High moisture content is found in traditional wooden construction, namely, carvel and clinker (also known as lapstrake), where planks are left exposed to the environment. Indeed, carvel relies on caulked seams to cope with the swelling of planks with increasing moisture content, while clinker construction employs overlapping planks (Birmingham, 1992; Gerr, 2000). In both cases, the swelling of the planks due to the high moisture content is necessary to achieve a watertight hull.

The past decade has seen a regain of interest in historical wooden boats and their analysis using modern naval architecture techniques (Rose, 2014; Souppez, 2016; Thomas and Souppez, 2018; Cannon et al., 2021; Souppez, 2021a; Loscombe, 2022; Loscombe, 2024). This is further evidenced in the development of modern replicas (Souppez, 2015; Alessio et al., 2016; White and Pereira, 2017; Alessio, 2017; Martus, 2018; Castro Ruiz and Perez Fernandez, 2020), new builds (Guell and Souppez, 2018; Scekic, 2018) and wooden cargo vessels (De Bleukelaer, 2018; Linden and Souppez, 2018; Armanto, 2019, Khan et al., 2021). Yet, there remains a lack of regulations to support the adoption of traditional wooden boatbuilding techniques for sustainability purposes (Loscombe, 2003; Truelock et al., 2022; Wang and Pegg, 2022, Souppez, 2023b) leading to new considerations for the regulatory implications of timber constructions (Meulemeester, 2018; Souppez, 2020) and regulatory compliance (Bucci et al., 2017; Souppez, 2021a).

Pre-1950 designs, whether original historical crafts or replicas built predominantly with the original materials, are beyond the scope of legislation (European Parliament, 2013; UK government 2017, Souppez, 2019) and associated structural regulations, e.g. ISO 12215-5:2019 (ISO, 2019a). In fact, regulatory frameworks primarily focus on modern wooden construction (Loscombe, 1998; Loscombe, 2003). While plank thicknesses are provided for a given estimated shell area by Germanischer Lloyd (GL, 2003), where the thickness-to-span ratio $t/s \approx 0.1$ for all ship sizes, only the American Bureau of Shipping (ABS, 2023) features traditional construction with dedicated scantling calculations. However, the ABS regulation does not account for the specifics of carvel construction, namely, closely spaced transverse members and mechanical fastening, which remain significant obstacles to the development of new regulations to support the adoption of traditional construction methods.

In this work, the transverse members are referred to as frames, a term employed in structural regulations (GL, 2003), and both carvel and clinked construction are commonly referred to as ‘plank-on-frame’. Other suitable terminology for the transverse frames under consideration may include timbers, ribs, doubler plates or stiffenening members.

Firstly, structural regulations are based on two assumptions, namely that panels are treated as built-in beams (100% end fixity), and the load is considered uniformly distributed (Souppez, 2021b). The first assumption may not be relevant to traditional construction, which features closely spaced small frames, and, thus, potentially a lower end fixity. Interestingly, recent developments in carbon fibre racing yachts have featured similar structures: small, closely spaced frames, where panels have been assumed to be simply supported (Harris, 2020; Lorimer, 2022). Additionally, with short panels, a robustness criterion may be relevant, which would lead to a point load instead of a uniformly distributed load. The combination of both changes to the regulatory assumption would result in a change in the maximum bending moment from $Ps^2/12$ for a built-in beam under uniformly distributed load, to $Ps^2/4$ for a simply supported beam subject to a central point load assumed as Ps. The new plating thickness t as a function of the design stress σ_{d} would, therefore, become

$$t = s\sqrt{\frac{1.5P}{\sigma_{\mathrm{d}}}}, \quad (1)$$

in lieu of the current

$$t = s\sqrt{\frac{0.5P}{\sigma_{\mathrm{d}}}}. \quad (2)$$

A thickness increase of $\sqrt{3}$ would, therefore, result from a change in underpinning assumptions. However, an additional failure mode may also need to be considered, namely shear. Indeed, given the high thickness and short span, panels with a higher thickness-to-span ratio would be achieved for carvel compared to modern wooden constructions such as cold moulding, strip planking and plywood (Souppez, 2023a). The mechanical testing of samples to determine shear properties under ISO 14130:1998 (ISO, 1998) is to be performed for $t/s = 0.100$. Conversely, flexural tests under ISO 178:2019 (ISO, 2019b) are to be conducted at $t/s = 0.050$, while four-point bending tests of timber beams under ISO 408:2010 (ISO, 2010) are to be undertaken at $0.0476 \leq t/s \leq 0.0556$. Carvel planking may, therefore, fail under shear, which is overlooked by current regulations. Additionally, the ratio of the ulitame shear strength to ultimate flexural strength may also be considered, with a value of 0.138 given in the ISO 12215-5 (ISO, 2019)

Secondly, carvel planks rely on a large number of mechanical fasteners, typically riveted copper nails (Birmingham, 1992). These require the use of a pilot hole and are counterbored, thereby introducing both a loss of material, and a stress concentration, none of which is currently accounted for despite empirical methods being available for their analysis (Young et al., 2012). Additionally, the pull force (or withdrawal force) exerted on a nail can be computed (Jones, 1989; Hoadley, 2000), though it is unlikely to be of concern. However, because the built-in end fixity of traditional construction may be questioned and simply supported may be seen as more suitable, the prying action may be critical. Indeed, contrarily to built-in beams, simply supported ones experience a slope at their support. This would cause a prying moment on nails (van de Lindt and Dao, 2009).

The mechanical testing of mechanically fastened carvel planks featuring closely spaced frames could provide novel insights into the failure behaviour of such planks and the effect of fasteners as well as frame spacing. This is crucial to furthering our understanding of traditional timber structures and may inform the recent developments in composite racing yacht structural arrangements inspired by the traditional closely spaced frames. However, such experimental data is not yet available. Consequently, four-point bending testing of carvel planks for a range of frame spacing is undertaken in line with ISO 408:2010 (ISO, 2010) to investigate the effect of mechanically fastened, closely spaced frames on timber planks. Furthermore, the effect of the thickness-to-span ratio is investigated.

The remainder of this paper is structured as follows. Section 2 details the timber beams investigated, the experimental setup and protocol, and the quantification of the mechanical properties and associated uncertainty. Then, Section 3 presents the findings associated with the effects of frames and thickness-to-span ratio. Finally, the main results are summarised in Section 4.

2. METHODOLOGY

2.1 TIMBER BEAMS

All beams were American White Oak (*Quercus alba*) with a physical density $\rho = 769$kg m^{-3} ± 82 kg m^{-3} at a moisture content $M_c = 11.7\% \pm 0.2\%$, quantified using a moisture meter. The planks were 700 mm long, ensuring appropriate overhangs were provided for the intended 600 mm span. The width $b = 50$ mm is dictated by the width of the support points, and the thickness $h = 20$ mm is consistent with previous work (Souppez, 2021a) and small craft plank thicknesses (Gerr, 2005). The frames are square sections 20 mm wide by 20 mm high, and extended the whole 50 mm of the plank width. All components were cut to size by the supplier. The plank and frame dimensions, together with the timber orientation, are depicted in Figure 1. Frames are fastened to the planking using 12 gauge, square section boat nails (2.65 mm by 2.69 mm cross section, 50.8 mm long including head), and 11.11 mm (7/16 inch) copper roves. Two copper nails are employed per frame, located 10 mm from the plank's edges.

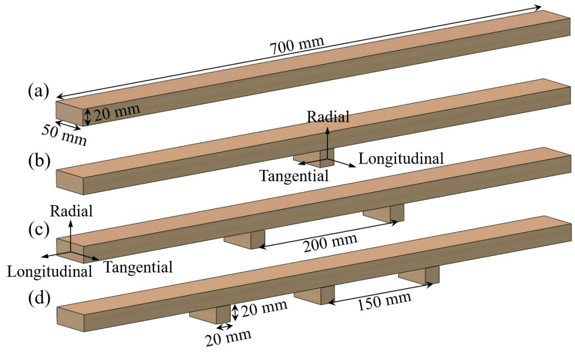

Figure 1: Schematics of the tested planks, with (a) no frame, (b) one frame, (c) two frames, and (d) three frames (copper nails omitted for clarity).

To understand the effect of the frames, four different plank configurations are tested, featuring:

- no frame, see Figure 1(a), and thus acting as a control experiment, with a centerline spacing $s_{\mathrm{CL}} = s = 600$ mm;
- one central frame, with $s_{\mathrm{CL}} = 300$ mm, see Figure 1(b);
- two frames, yielding $s_{\mathrm{CL}} = 200$ mm, see Figure 1(c); and
- three frames, such that $s_{\mathrm{CL}} = 150$ mm, see Figure 1(d).

Additionally, further experiments are undertaken on planks without frames to investigate the effect of the thickness-to-span ratio t/s. Two thicknesses are investigated, $t = 20$ mm and $t = 8$ mm, the former at $s =$ 600 mm, 300 mm, 200 mm and 100 mm, and the latter at $s =$ 300 mm, 200 mm, 100 mm and 80 mm.

2.2 EXPERIMENTAL SETUP

All experiments were undertaken on an Instron 5965 equipped with a 5 kN load cell. The four-point bending setup, with a support-to-load span $s/l = 3$, in line with ISO 408:2010 (ISO, 2010), is depicted in Figure 2. All support and loading points have a radius $r = 5$ mm. Experiments were undertaken at temperatures 19.7 °C $\leq T \leq$ 21.4 °C and relative humidies $0.37 \leq \varphi \leq 0.44$. Before the data is recorded at 100 Hz, a 1 N preload is applied at a displacement rate of 2 mm min^{-1}, following which the tests are conducted at 0.06 mm s^{-1}, or $0.003h$ as defined in ISO 408:2010 (ISO, 2010), equivalent to 3.6 mm min^{-1}.

Figure 2: Four-point bending setup with $s/l = 3$.

2.3 MECHANICAL PROPERTIES

From the measured force F and cross-head displacement ω (which is also the beam deflection at the one-third span points) the maximum strain ε for $s/l = 3$ are respectively given by

$$\sigma = \frac{Fs}{bh^2}, \tag{3}$$

obtained from the maximum bending moment of $Fs/6$ divided by the minimum section modulus of $bh^6/6$ and

$$\varepsilon = \frac{4.7h\omega}{s^2}. \tag{4}$$

The flexural modulus E is then computed as

$$E = \frac{\sigma}{\varepsilon}, \tag{5}$$

using the linear least squares method for a strain range $0.001 \leq \epsilon \leq 0.005$, which is the approximate limit of proportionality strain as shown in Figure 3

2.4 UNCERTAINTY QUANTIFICATION

The uncertainty quantifies the equipment, sample and wood variability error at the 95% confidence level. This pessimistic approach is intended to ensure safe and reliable conclusions are reached.

The uncertainty U of the present results is given as

$$U = \sqrt{(B^2 + P_{\mathrm{r}}^2)}, \tag{6}$$

where the bias $B(X)$ of a quantity X based on a number N of independent variables x_i with a bias limit $B(x_i)$, as given in Table 1, is

$$B(X) = \sqrt{\sum_{i=1}^{N}\left(\frac{\partial X}{\partial x_i}B(x_i)\right)^2}, \tag{7}$$

and the precision P_r based on the standard deviation σ_{dev} at the 95% confidence level $t_{95} = 2.776$ for the number of repeats $n = 5$ undertaken is

$$P_r = \frac{t_{95}\sigma_{\mathrm{dev}}}{\sqrt{n}}. \tag{8}$$

Table 1: Summary of bias limits.

Span, $B(s)$	0.5 mm
Force, $B(F)$	0.00005 N
Width, $B(b)$	0.005 mm
Thickness, $B(t)$	0.005 mm
Deflection, $B(\omega)$	0.00005 mm

3. RESULTS

3.1 FRAME SPACING

3.1 (a) Stress-Strain Curves

The stress-strain curves of the various configurations investigated at $s = 600$ mm are present in Figure 3, namely no frame in Figure 3(a), one frame in Figure 3(b) two frames in Figure 3(c) and three frames in Figure 3(d). Qualitatively, these results yield two main findings.

First, the plank failure is primarily abrupt. When no frames are present, the failure consistenlty occurs between the loading points, where the bending moment is constant and at its maximum. For planks with frame, the failures occurred at a frame location in all but two cases for the one frame configuration, and all but one case for the two and three frames configurations, respectively. In these cases, however, the failure occurred close (with 30 mm) of the frame, and between loading point. This suggests the introduction of the frames and associated holes which reduce the local section modulus of the plank promotes failure at these locations, with a few exceptions where local wood defects induced failure where the maximum bending moment was applied.

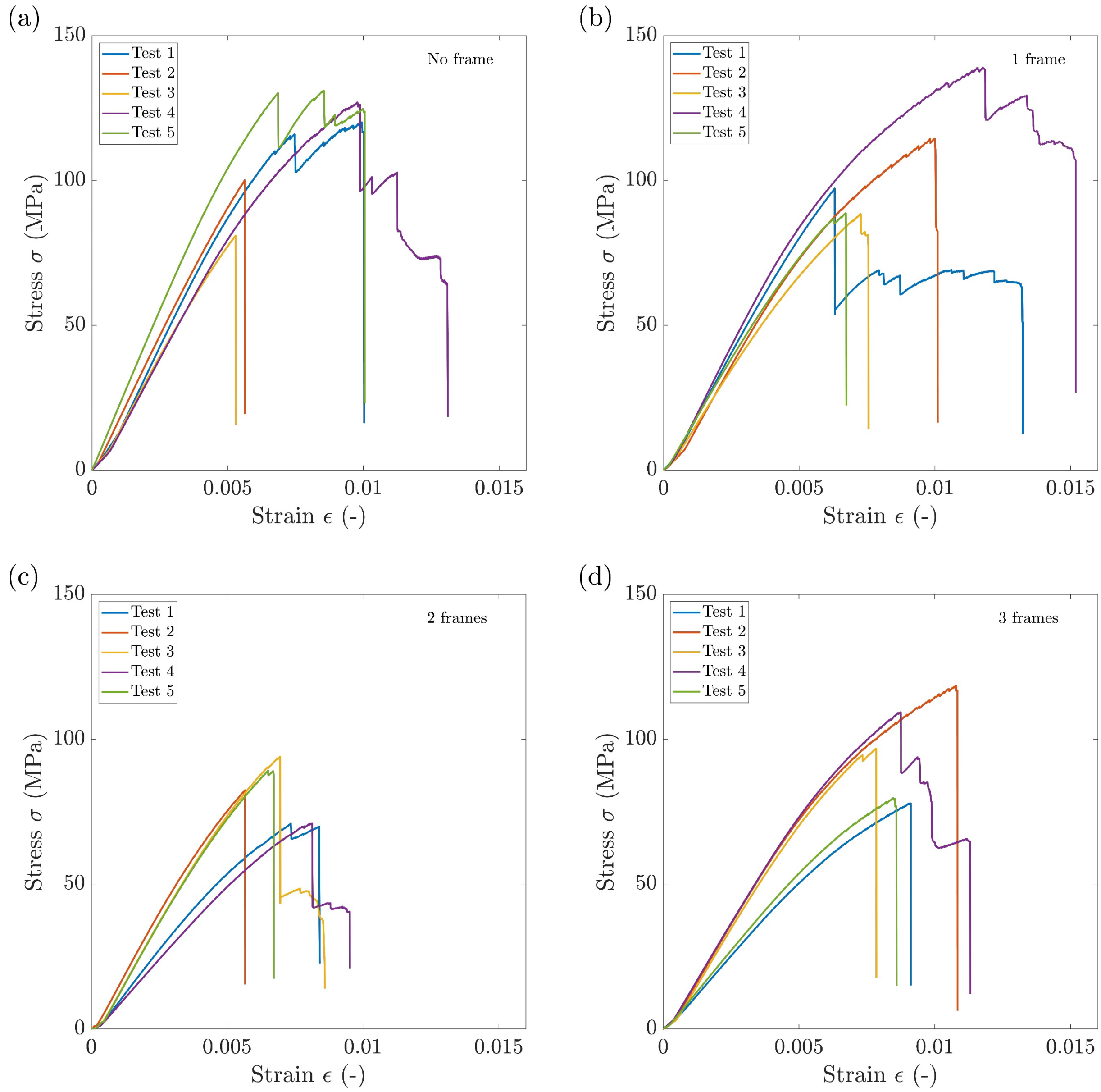

Figure 3: Stress-strain curves for the five repeats ($n = 5$) of the four-point bending tests with (a) no frame ($s_{\mathrm{CL}} = 600$ mm), (b) 1 frame ($s_{\mathrm{CL}} = 300$ mm), (c) 2 frames ($s_{\mathrm{CL}} = 200$ mm) and (d) 3 frames ($s_{\mathrm{CL}} = 150$ mm).

Secondly, there is marked reduction in the maximum stress and strain experienced by planks with two frames, i.e. $s_{\mathrm{CL}} = 200$ mm. Because of the four-point bending setup, where $s/l = 3$, the two frames are directly underneath the loading points. Here, it is hypothesised this may cause the early failure, and is associated with a stress-raiser event, as further discussed in Sections 3.1(b) and 3.1 (c) for the stiffness and strength, respectively.

3.1 (b) Stiffness

The flexural modulus E is quantified for all configurations and presented in Figure 4, together with ISO 12215-5:2019 (ISO 2019a) estimation for hardwood, namely, $E = 0.0175\rho$. Indeed, the mechanical properties of a timber species can be directly related to its density. Consequently, Figure 4 also presents the specific modulus E/ρ to account for the variations in timber densities between the various planks investigated in this work. Further variations in the properties of timber are captured by the error bars, thanks to the uncertainty analysis of the results (see Section 2.4) to ensure the results are not affected by the natural variations in timber properties.

The four values of s_{CL} investigated cover the expected range of frame spacing for small crafts (Gerr, 1999). Thus, generalised conclusions are drawn from the results obtained. There is a notable and monotonic increase in modulus with the frame spacing for the range considered. The specific modulus displays a similar trend, albeit with a local minimum at $s_{\mathrm{CL}} = 200$ mm (two frames), which is attributed to the alignment between loading points and the frames and associated stress raiser. While ISO 12215-5:2019 (ISO, 2019a) only features a strength-based criterion for planking thickness, the comparison between the experimental values and ISO default properties remains of interest.

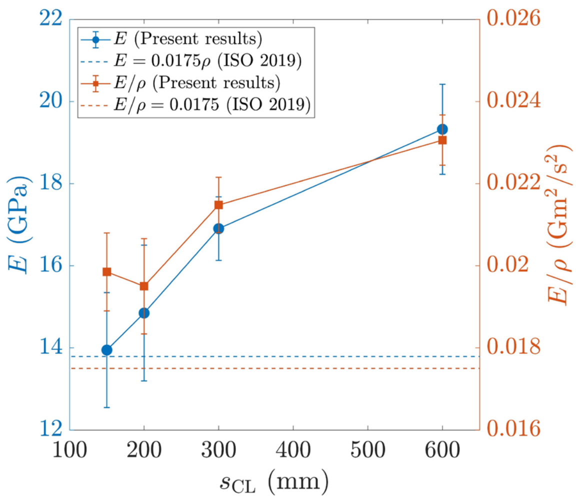

Figure 4: Modulus E and specific modulus E/ρ for planks with no frames ($s_{\mathrm{CL}} = 600$ mm), one frame ($s_{\mathrm{CL}} = 300$ mm), two frames ($s_{\mathrm{CL}} = 200$ mm) and three frames ($s_{\mathrm{CL}} = 150$ mm) ($n = 5$).

Here, it should be noted that, while the results are reported as the average value from the five repeats, with the error bars quantifying the uncertainty (see Section 2.4), the mechanical properties derived from experimental testing should be derated to be the lesser of 80% of the average, of the average minus two standard deviations. For the present results, this roughly coincides with the lower bound of the error bars. Consequently, while the specific modulus values consistently exceeded the ISO default value, the uncertainty associated with timber density means that the modulus of the tested planks is below the ISO default value for $s_{\mathrm{CL}} \leq 200$ mm. This is significant as, for small boats, $s_{\mathrm{CL}} = 150$ mm (circa 6 inch) is commonly employed (Birmingham, 1992), and thus ISO 12215-5:2019 (ISO, 2019a) may overestimate the modulus.

Caution is advised when looking at the results of Figure 4. Indeed, while the effective effect of the number of transverse frame for a given span have been quantified, a physical explanation remains to be theorised. The variations are not thought to arise from the variability of wood testing. However, whether they should be attributed to the presence of the frame (which are small comparative to the beam, with each frame having a width $b = 0.0333s$), or the presence of holes for the copper rivets (reducing the section modulus of the beam) is yet to be ascertained, and will be discussed when exploring areas of future work in the Conclusions (Section 5).

3.1. (c) Strength

The ultimate flexural strength σ and associated specific strength σ/ρ are presented in Figure 5. First, a significant reduction in both σ and σ/ρ is evidenced at $s_{\mathrm{CL}} = 200$ mm (two frames). Because of the associate stress raiser, this data point and considering the magnitude of the error bars, σ/ρ appears independent of the frame spacing. However, in all cases, the lower bound of the error bars is below the default value of ISO 12215-5:2019 (ISO, 2019a), namely, $\sigma = 0.130\rho$.

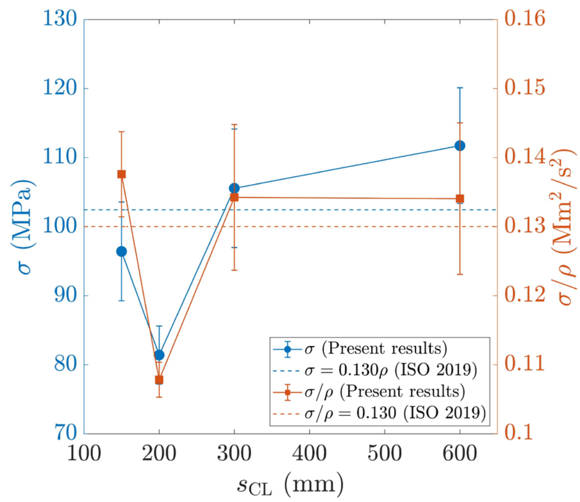

Figure 5: Strength σ and specific strength σ/ρ for planks with no frames ($s_{\mathrm{CL}} = 600$ mm), one frame ($s_{\mathrm{CL}} = 300$ mm), two frames ($s_{\mathrm{CL}} = 200$ mm) and three frames ($s_{\mathrm{CL}} = 150$ mm) ($n = 5$).

As the planking thickness is solely driven by a strength criteria in ISO 12215-5:2019 (ISO, 2019a), as previously introduced in Equation (2), where $\sigma_{\mathrm{d}} = \sigma$ for timber construction, an additional factor of safety would be needed for traditional wooden boatbuilding methods, such as carvel planking, to be safely included in the scope of existing regulations. However, the fact that s_{CL} does not impact σ/ρ would suggest that, providing suitable factors of safety are in place, the frame spacing would not be an issue. This would be valid only for failure in flexion, as opposed to shear. Consequently, the effect of the thickness-to-span ratio is investigated next to ascertain if there exists a change in failure behaviour for high t/s, which is characteristic of traditional wooden boatbuilding.

3.2 THCKNESS-TO-SPAN RATIO

3.2 (a) Stiffness

Four-point bending experiments on planks without frames are undertaken to characterise the effect of t/s on flexural properties. Two plank thicknesses are investigated in this work, namely, $t = 20$ mm for 100 mm $\leq s \leq 600$ mm and $t = 8$ mm for 80 mm $\leq s \leq 300$ mm. Figure 6 presents the variations in E and E/ρ with t/s. Here, E represents an apparent modulus, i.e. assuming that the deflection is solely driven by bending. A true modulus could only be estimated in the absence of an experimental value for the shear modulus. However, it is expected that a true value of E, accounting for shear deflection, would yield a less sever decline in E with t/s as greater shear deflection would be expected for higher values of t/s.

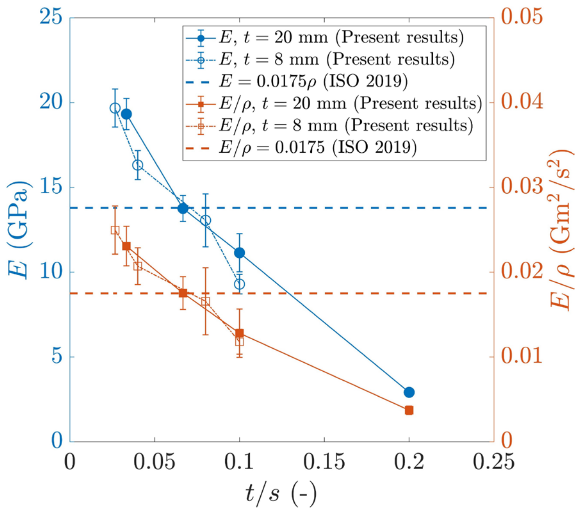

Figure 6: Modulus E and specific modulus E/ρ for $t = 20$ mm and $t = 8$ mm planks ($n = 5$).

For both thicknesses, an identical trend showcasing a monotonic decrease in E and E/ρ with increasing t/s is evidenced. Remarkably, the cross-over between the lower bound of the error bars of the present experimental results and ISO 12215-5 (ISO, 2019a) default modulus occurs for $0.050 < t/s < 0.100$, with values exceeding the default one for $t/s \leq 0.050$, and values lower the default one for $t/s \geq 0.100$. This is consistent with the requirements of ISO 14130:1998 (ISO, 1998) to undertake shear experiments at $t/s = 0.100$, while for flexion ISO 178:2019 (ISO, 2019b) imposes $t/s = 0.050$ for composites and ISO 408:2010 (ISO, 2010) dictates $0.0476 \leq t/s \leq 0.0556$ for timber. Therefore, and while there is no step change in E and E/ρ with t/s but rather a gradual decline as t/s increases, the present results clearly identify t/s as a critical value. This is very relevant to traditional construction where thick planks and closely spaced frames yield high values of t/s that ISO 12215-5:2019 (ISO, 2019a) does not appear suited for. Whether the same conclusion can be drawn for the strength is ascertained in the following subsection.

3.2 (b) Strength

By reducing the span to investigate the effect of t/s, a higher breaking load is required, which is limited to 5 kN due to the instrumentation employed (see Section 2.2). Consequently, while a modulus could be assessed for all experiments in Section 3.2(a), the ultimate flexural strength is only available for $t = 20$ mm at $s = 600$ mm, as shorter spans did not achieve failure. For all $t = 8$ mm experiments, ultimate flexural strength values are reported for all values of s investigated. The results for the strength and specific strength at thickness-to-span ratios $0.0267 \leq t/s \leq 0.100$ are presented in Figure 7. As for the stiffness, an apparent σ is calculated here, assuming a solely bending-driven flexion, which is unlikely to hold for higher values of t/s.

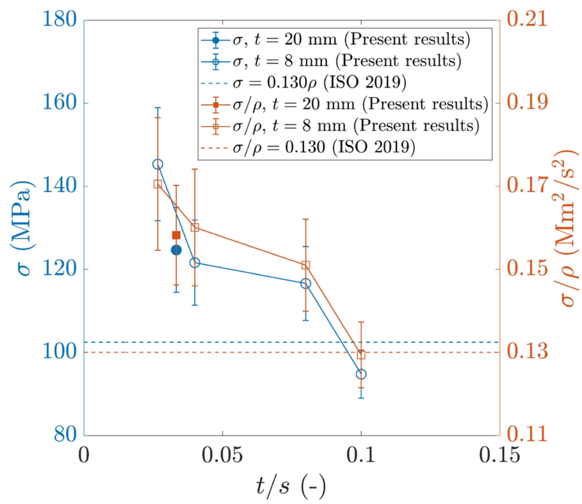

Figure 7: Strength σ and specific strength σ/ρ for $t = 20$ mm and $t = 8$ mm planks ($n = 5$).

These results are explained by the bending-shear stress interaction, with studies such as that of Schneeweiß and Felber (2013) and Danawade et al. (2014) showcasing the need for a suitable t/s ratio for correct flexural properties to be exhibited. Given the previously evidenced strong agreement between E and E/ρ (see Figure 6) and strong agreement between the data point at $t = 20$ mm and the trend displayed at $t = 8$ mm, the results presented in Figure 7 can be generalised to higher thicknesses than $t = 8$ mm. Similar to the E and E/ρ in Figure 6, the lower bound of the error bars for σ and σ/ρ in Figure 7 exhibit a cross-over with ISO 12215-9:2019 (ISO, 2019a) default values for $0.050 < t/s < 0.100$, albeit towards the higher end of that range. Indeed, for $t/s \leq 0.080$, both σ and σ/ρ exceed their default regulatory values.

This further confirms the importance of t/s in ensuring existing regulations for small craft structures can be safely applied to traditional wooden boats. Given the strength based criterion of ISO 12215-5:2019 (ISO, 2019a) and the present results evidencing overestimated properties for $t/s > 0.080$, this value should not be exceeded unless additional factors of safety are implemented.

The specified threshold is particularly relevant as, for small both, combining the planking thickness and frame spacing recommended by Gerr (2000) yields

$$t/s = 0.0728\, S_\mathrm{n}^{0.13}, \tag{9}$$

where S_n is the scantling number, given as

$$S_\mathrm{n} = \frac{L_\mathrm{OA} B_\mathrm{H} D_\mathrm{H}}{28.32}, \tag{10}$$

with L_OA being the length overall, B_H the hull beam and D_H the hull depth.

Gerr (2000) considers $0.04 \le S_\mathrm{n} \le 32$. For values $0.04 \le S_\mathrm{n} \le 2$, then $0.0479 \le t/s \le 0.0797$, i.e. consistently below the maximum strength threshold of $t/s = 0.080$. However, for the vast majority of boats where $2 \le S_n \le 32$, t/s would always exceed 0.080. Moreover, for any size boat, the value of t/s would exceed the maximum 0.050 defined soft stiffness in Section 3.2 (a). Consequently, an additional factor of safety may be required to ensure existing regulations can be made suitable for traditional wooden boats under current regulations.

3.3 MOISTURE CONTENT

For boatbuilding applications, moisture content ranges from 7% (kiln-dried) to 14% (air-dried) (Hoadley, 2000), with 7% to 16% allowed in ABS (2023) and 8% to 14% in GL (2004). For modern boatbuilding, the epoxy encapsulation means the timber will remain within this moisture content throughout the operating life of the vessel. However, for traditional construction, the moisture content would increase up to 28%-30%, also known as the fibre saturation point (Barkas, 1935), while in the water. This is necessary for both carvel and clinker to achieve a watertight hull, but this increase in moisture content has consistently been associated with a sharp reduction in material properties (Babiak et al., 2018; Bader and Nemeth, 2019; Korkmaz and Buyuksari, 2019; Fu et al., 2021).

Mechanical properties for timber are typically given at 12% moisture content, as is the case in ISO12215-5:2019 (ISO, 2019a), and is consistent with the present work undertaken on American White Oak samples with a moisture content 11.7% ± 0.2%. At the fibre saturation point, a reduction in strength of circa 46% compared to 12% moisture content would be expected for Oak based on the work of Korkmaz and Buyuksari (2019). Similarly, a 50% reduction in the modulus of Oak between 12% moisture content and the fibre saturation point was evidenced by Babiak et al. (2018). This would imply that the factor of safety of the mechanical properties of timber for traditional construction, operating at fibre saturation point would need to be at least doubled compared to current regulations to ensure their safe application. Another consideration might be to employ the mechanical properties of timber at saturation (>30% moisture content).

4. CONCLUSIONS

Four-point bending tests were undertaken on American White Oak planks for a range of thicknesses, spans, and with up to three riveted frames in order to replicate carvel planking. The aim was to understand the effect of both frames and the thickness-to-span ratio on the strength and stiffness of traditional wooden boat structures to evaluate the applicability of existing small craft structural regulations.

First, the results showed that, for a given span, an increase in the number of frames leads to a sharp decline in specific stiffness but not specific strength. However, the latter proved to be below the assumed regulatory properties. Additionally, the results revealed a significant occurrence of failure at the location of a riveted frame, while the interaction between the loading points and stinger location was noted and yielded too pessimistic a specific strength.

Secondly, the thickness-to-span ratio was shown to negatively affect both the specific strength and stiffness, i.e. a large value of the thickness-to-span ratio, as commonly found on carvel construction, leads to a reduction in mechanical properties. In order to exceed the regulatory strength and stiffness for carvel planks, a maximum ratio of 0.080 and 0.050 is recommended, respectively. However, it is noted that the higher moisture content associated with traditional boatbuilding would lead to a significant loss of mechanical properties and, thus, would warrant the inclusion of additional factors of safety to ensure the safety and regulatory compliance of traditionally built wooden vessels.

These findings provide novel insights into the structural design and performance of tradional carvel planking with riveted frames, and may contribute to future developments in wooden and composite structural design, as well as support the application of future structural regulations to traditional crafts, for both historical and sustainability purposes.

Future work, however, remains to be undertaken to gain further understanding of the physics behind the present results. As such, the following recommendations are made:

(1) For beams to be tested with adhesively bonded frames, as opposed to rivetted ones. This will enable to assess whether it is the presence of the frames of the riveting holes that yields a reduction in mechanical properties.

(2) Additionally, testing of beams with the rivet holes drilled but no rivets or frames will further confirm if the loss of section modulus is the cause of the change in mechanical properties.

(3) Experiments could also be conducted on the same beams (with loading kept well within the elastic region), to alleviate any concerns the variations in mechanical properties observed originate from the variability in timber (grain orientation, mosture content, density, etc…).

(4) The absence of an experimental value for the shear modulus limits the ability to compute the true modulus and strength (Figures 6 and 7). Experiments dedicated to quantifying the shear modulus would, therefore, contribute to a further level of analysis of the present results.

(5) Lastly, experiments have been conducted on individual beams. These would normally be further supported or constrained at their edges, introducing a variation between carvel and clinker construction. Therefore, the testing of carvel and clinked panel would be seen as a relevant area of future work.

5. REFERENCES

1. ALESSIO, L G., (2017). *Redesign of a classic sailboat with FEA investigation of the plate curvature*. MSc Thesis, University of Liege, Liege, Belgium.
2. ALESSIO, L., SOUPPEZ, J.-B. R G., and HAGE, A. (2016). D*esign evaluation and alteration of the Dark Harbor 17.5: case study of a modern replica*. RINA Historic Ships, London, UK.
3. AMERICAN BUREAU OF SHIPPING (2023). *Rules for building and classing - Yachts - Part 3 hull construction and equipment.* American Bureau of Shipping, Spring, Texas, US.
4. ARMANTO, J. (2019). *The future of sailing cargo.* Thesis, University of Turku, Turku, Finland.
5. BABIAK, M., GAFF, M., SIKORA, A. and HYSEK, Š. (2018). *Modulus of elasticity in three-and four-point bending of wood.* Composite Structures. 204: 454-465. https://doi.org/10.1016/j.compstruct.2018.07.113
6. BÁDER, M., and NÉMETH, R. (2019). *Moisture-dependent mechanical properties of longitudinally compressed wood.* European Journal of Wood and Wood Products. 77: 1009-1019. https://doi.org/10.1007/s00107-019-01448-1
7. BARKAS, W. W. (1935). *Fibre saturation point of wood*. Nature. 135: 545. https://doi.org/10.1038/135545b0
8. BAXTER, J. P. (1933). *The introduction of the iron-clad warship*. Harvard University Press: Harvard, US.
9. BECK, R., BOOTE, D., DAVIES, P., HAGE, A., HUDSON, D., KAGEYAMA, K., KEUNING, J.A. and MILLER, P. (2009). *Sailing yacht design.* 17th International Ship and Offshore Structures Congress, Seoul, Korea.
10. BIRMINGHAM, R. (1992) *Boat building techniques illustrated.* London, UK: Adlard Coles Nautical; 2nd edition.
11. BUCCI, V., CORIGALIANO, P., EPASTO, G., GUGLIELMINO E. and MARINO, A. (2017). *Experimental investigation on iroko wood used in shipbuilding*. Institution of Mechanical Engineers, Part C, Journal of Mechanical Engineering Science. 231(1): 128-139. https://doi.org/10.1177/095440621667449
12. CANNON, S. BOYD, S. and WHITEWRIGHT, J. (2019). D*evelopment of a quantitative method for the assessment of historic ship performance*. 14th International Symposium on Practical Design of Ships and Other Floating Structures, PRADS 2019, Yokohama, Japan.
13. CASTRO RUIZ, M., and PEREZ FERNANDEZ, R. (2020). *Galatea II: Reborn of a classic*. RINA Historic Ships, London, UK.
14. DANAWADE, B.A., MALAGI, R.R., KALAMKAR, R.R. and SARODE, A.D. (2014). *Effect of span-to-depth ratio on flexural properties of wood filled steel tubes.* Procedia Materials Science. 5, pp.96-105.
15. DE BEUKELAER, C. (2018). *Plain Sailing: How Traditional Methods could Deliver Zero-Emission Shipping.* The Conversation.
16. EUROPEAN PARLIAMENT (2013). D*irective 2013/53/EU on recreational craft and personal watercraft*. Official Journal of the European Union, Luxembourg, Luxembourg.
17. FAIRBAIRN, W. (1865). *treatise on iron ship building: Its history and progress as comprised in a series of experimental researches on the laws of strain.* Longmans, Green & Company.
18. FU, W.-L., GUAN, H.-Y. and KEI, S. (2021). *Effects of moisture content and grain direction on the elastic properties of beech wood based on experiment and finite element method.* Forests. 12(5): 610. https://doi.org/10.3390/f12050610
19. GERMANISCHER LLOYD (2003). *Rules for classification and construction - I Ship technology - 3 Special craft - 3 Yachts and boats up to 24 m.* Germanischer Lloyd, Hamburg, Germany.

20. GERR, D. (2000). *The elements of boat strength: for builders, designers, and owners.* International Marine/McGraw-Hill New York, United States.
21. GOUGEON, M. (2005). *The Gougeon brothers on boat construction.* Bay City, Michigan, US: Gougeon Brothers Incorporated.
22. GREENE, E. (1990). *Use of fiber reinforced plastics in the marine industry*. Ship Structure Committee, National Academy of Science, Washington DC, United States.
23. GUELL, A. and SOUPPEZ, J.-B. R. G. (2018). *Combining modern hydrofoils with wooden classic*. British Conference of Undergraduate Research, Sheffield, UK.
24. HARRIS, S. P. H. (2020). *Structural design, sizing and optimisation for a foiling monohull.* Thesis, The University of Auckland, Auckland, New Zealand.
25. HOADLEY, R. B. (2000). U*nderstanding wood: a craftsman's guide to wood technology.* Newtown, Connecticut, United States: Taunton Press.
26. INTERNATIONAL ORGANIZATION FOR STANDARDIZATION (1998). *ISO 14130:1998 - Fibre-reinforced plastic composites - Determination of apparent interlaminar shear strength by short-beam method.* International Organization for Standardization, Geneva, Switzerland.
27. INTERNATIONAL ORGANIZATION FOR STANDARDIZATION (2010). *BS EN 408:2010 Timber structures – Structural timber and glued laminated timber – Determination of some physical and mechanical properties*. International Organization for Standardization, Geneva, Switzerland.
28. INTERNATIONAL ORGANIZATION FOR STANDARDIZATION (2019a) *ISO 12215-5:2019 Small craft - Hull construction and scantlings - Part 5: Design pressures for monohulls, design stresses, scantlings determination.,* International Organization for Standardization, Geneva, Switzerland.
29. INTERNATIONAL ORGANIZATION FOR STANDARDIZATION (2019b). *ISO 178:2019 - Plastics - Determination of flexural properties.* International Organization for Standardization, Geneva, Switzerland.
30. JONES, T. H. (1989). *The encyclopedia of wood.* New York, US: Sterling Publishing Co INC International Concepts.
31. KHAN, L., MACKLIN, J J. R., PECK, B. C. D., MORTON, O. and SOUPPEZ, J.-B. R. G. (2021). *A review of wind-assisted ship propulsion for sustainable commercial shipping: Latest developments and future stakes.* RINA Wind Propulsion Conference, London, UK.
32. KORKMAZ, O., and BÜYÜKSARI, Ü. (2019). *Effects of moisture content on mechanical properties of micro-size oak wood.* BioResources. 14(4): 7655-7663. http:\\www.doi.org/10.15376/biores.14.4.7655-7663
33. LINDEN, V. and SOUPPEZ, J.-B. R. G. (2018). *Sailing towards sustainable trading with wooden cargo schooner.* British Conference of Undergraduate Research, Sheffield, UK.
34. LORIMER, T. and T. ALLEN (2022). *Concurrent multi-component optimization of stiffened-plate yacht structures.* Journal of Sailing Technology. 7(1): 203-227. https://doi.org/10.5957/jst/2022.7.10.203
35. LOSCOMBE, P. R. (1998). S*tructural design considerations for laminated wood yachts.* International Conference on the Modern Yacht, Portsmouth, UK.
36. LOSCOMBE, P. R. (2003). *Developing an iso scantling standard for recreational craft of laminated wood constructio*n. The Modern Yacht Conference, Southampton, UK.
37. LOSCOMBE, P. R. (2022). *Analysing ancient (viking) longship structure*. International Journal of Maritime Engineering. 164(A2): 207-220. https://doi.org/10.5750/ijme.v164iA2.1170
38. LOSCOMBE, P. R. (2024). *Some observations on the strength of viking ship rudders.* Preprint - International Journal of Maritime Engineering, 2024.
39. MARTUS, V. (2018). *Major refit of a sailing replica of the 18th century frigate experience and traditional skills obtained by a team of volunteers*. RINA Historic Ships, London, UK.
40. MCGRAIL, S. (2014). *Ancient boats in north-west europe: The archaeology of water transport to AD 1500*. Routledge, Milton Park, UK.
41. MEULEMEESTER, D. (2018). *The classification of historic(al) vessels and their replicas.* RINA Historic Ships, London, UK.
42. PARK, G., KIM, J.-C., YOUN, M., YUN, C., KANG, J., SONG, Y.-M., SONG, S.-J., NOH, H.-J., KIM, D.-K., and IM, H.-J. (2010). *Dating the bibong-ri neolithic site in korea: Excavating the oldest ancient boat.* Nuclear Instruments and Methods in Physics Research Section B: Beam Interactions with Materials and Atoms. 268(7-8): 1003-1007. https://doi.org/10.1016/j.nimb.2009.10.084
43. ROSE, K. J. (2014). *The naval architecture of vasa, a 17th-century swedish warship*. Doctoral Thesis, Texas A & M University, Colle Station, Texas, US.
44. SCEKIC, S. (2018). *Design of a 23 m modern-classic wooden sailing yacht with timber investigation.* MSc Thesis, University of Liege, Liege, Belgium.
45. SCHNEEWEIß, G. and FELBER, S. (2013). *Review on the bending strength of wood and influencing factors.* American Journal of Materials Science. 3(3), pp.41-45.

46. SOUPPEZ, J.-B. R. G. (2015). *Design and production of a wooden Thames A Rater class sailing yacht.* MEng Thesis, The University of Auckland, Auckland, New Zealand.
47. SOUPPEZ, J.-B. R. G. (2016). *On the applications of modern naval architecture techniques to historical crafts.* RINA Historic Ships, London, UK.
48. SOUPPEZ, J.-B. R. G. (2018). *Structural design of high performance composite sailing yachts under the new BS EN ISO 12215-5.* Journal of Sailing Technology. 3(1): 1-18. https://doi.org/10.5957/jst.2018.02
49. SOUPPEZ, J.-B. R. G. (2019). D*esigning the next generation of small pleasure and commercial powerboats with the latest iso 12215-5 for hull construction and scantlings*. First SNAME/IBEX Symposium, United States.
50. SOUPPEZ, J.-B. R. G. (2020). *Timber construction: an experimental assessment of the strength of scarf joints and the effectiveness of various adhesives for laminated wood.* RINA Historic Ships, London, UK.
51. SOUPPEZ, J.-B. R. G. (2021a). E*xperimental testing of scarf joints and laminated timber for wooden boatbuilding applications.* International Journal of Maritime Engineering. 163(A3): 185-193. https://doi.org/10.5750/ijme.v163iA3.16
52. SOUPPEZ, J.-B. R. G. (2021b). *Ships and Maritime Transportation*. In: Springer Handbook of Mechanical Engineering. Springer, Berlin, Germany, 1139-1164. https://doi.org/10.1007/978-3-030-47035-7_25
53. SOUPPEZ, J.-B. R. G. (2023a). *Structural design of wooden boats.* RINA Historic Ships Conference, London, UK.
54. SOUPPEZ, J.-B. R. G. (2023b). S*tructural challenges of low-emission vessels: A review.* International Journal of Maritime Engineering. 165(A2): 165-178. https://doi.org/10.5750/ijme.v165iA2.1233
55. THOMAS, J. and SOUPPEZ, J.-B. R. G. (2018). C*omparative performance prediction of historical Thames A Rater class designs*. RINA Historic Ships, London, UK.
56. TRUELOCK, D., LAVROFF, J., PEARSON, D., CZABAN, Z., LUO, H., WANG, F., CATIPOVIC, I., BEGOVIC, E., TAKAOKA, Y., LOUREIRO, C., SONG, C. Y., GARCIA, E., EGOROV, A., SOUPPEZ, J.-B. R. G., SENSHARMA, P., and NICHOLS-LEE, R. (2022). *Committee V.5: Special vessels.* 21st International Ship and Offshore Structures Congress, Vancouver, Canada.
57. UK GOVERNMENT (2017). *The recreational craft regulations 2017*. UK Government, London, UK.
58. VAN DE LINDT, J. W. and DAO, T. N. (2009). P*erformance-based wind engineering for wood-frame buildings*. Journal of Structural Engineering. 135(2): 169-177. https://doi.org/10.1061/(ASCE)0733-9445(2009)135:2(169)
59. WANG, X. and PEGG, N. (2022). *Proceedings of the 21st international ship and offshore structures congress volume 2 specialist committee reports.* 21st International Ship and Offshore Structures Congress, Volume 2, Vancouver, Canada.
60. WARD, C. (2006). *Boat-building and its social context in early egypt: Interpretations from the first dynasty boat-grave cemetery at Abydos*. Antiquity. 80(307): https://doi.org/10.1017/S0003598X00093303 118-129.
61. WHITE, R. G., and PEREIRA, R. S. (2016) *Lilian:From gentleman's yacht to scrap and back*. RINA Historic Ships, London, UK.
62. YOUNG, W. C., BUDYNAS, R. G., and SADEGH, A. M. (2012). R*oark's formulas for stress and strain*. New York, US: McGraw-Hill Education.